In Situ Imaging of *Candida albicans* Hyphal Growth via Atomic Force Microscopy

Arzu Çolak,[a*] Mélanie A. C. Ikeh,[b] Clarissa J. Nobile,[b] Mehmet Z. Baykara[a]

[a]Department of Mechanical Engineering, University of California Merced, Merced, California, USA
[b]Department of Molecular and Cell Biology, University of California Merced, Merced, California, USA

ABSTRACT *Candida albicans* is an opportunistic fungal pathogen of humans known for its ability to cause a wide range of infections. One major virulence factor of *C. albicans* is its ability to form hyphae that can invade host tissues and cause disseminated infections. Here, we introduce a method based on atomic force microscopy to investigate *C. albicans* hyphae *in situ* on silicone elastomer substrates, focusing on the effects of temperature and antifungal drugs. Hyphal growth rates differ significantly for measurements performed at different physiologically relevant temperatures. Furthermore, it is found that fluconazole is more effective than caspofungin in suppressing hyphal growth. We also investigate the effects of antifungal drugs on the mechanical properties of hyphal cells. An increase in Young's modulus and a decrease in adhesion force are observed in hyphal cells subjected to caspofungin treatment. Young's moduli are not significantly affected following treatment with fluconazole; the adhesion force, however, increases. Overall, our results provide a direct means of observing the effects of environmental factors and antifungal drugs on *C. albicans* hyphal growth and mechanics with high spatial resolution.

IMPORTANCE *Candida albicans* is one of the most common pathogens of humans. One important virulence factor of *C. albicans* is its ability to form elongated hyphae that can invade host tissues and cause disseminated infections. Here, we show the effect of different physiologically relevant temperatures and common antifungal drugs on the growth and mechanical properties of *C. albicans* hyphae using atomic force microscopy. We demonstrate that minor temperature fluctuations within the normal range can have profound effects on hyphal cell growth and that different antifungal drugs impact hyphal cell stiffness and adhesion in different ways.

KEYWORDS *Candida albicans*, atomic force microscopy, hyphal development

Candida albicans is a commensal of humans that asymptomatically colonizes the skin, oral cavity, and gastrointestinal and reproductive tracts of healthy individuals (1, 2). *C. albicans* is also one of the most common opportunistic fungal pathogens of humans that typically causes superficial mucosal infections (e.g., vulvovaginal candidiasis) in healthy individuals (3). In immunocompromised individuals (e.g., AIDS patients, cancer and chemotherapy patients, and organ and bone marrow transplantation patients), *C. albicans* can also cause life-threatening bloodstream infections (1, 4). An important virulence trait of *C. albicans* is its ability to form biofilms on mucosal surfaces and on implanted medical devices, such as vascular and urinary catheters, cardiac valves, artificial vascular bypass devices, pacemakers, ventricular assist devices, dentures, and joint prostheses (5, 6). Biofilms are communities of microbial cells attached to a substratum or formed at a liquid-air interface that are embedded in a matrix of extracellular polymeric substances (6, 7). Biofilms can be highly tolerant and resistant to antifungal agents and host defenses (8, 9). *C. albicans* biofilm formation is a multifaceted process that begins when unicellular round yeast-form cells adhere to a surface (9,

10). This is followed by formation of elongated hyphal and pseudohyphal cells along with the production of the extracellular matrix (9–11). Hyphal cells are essential for biofilm formation and maintenance because they provide architectural support to the biofilm structure (6). They are also critical for *C. albicans* cells to invade epithelial cell layers and cause tissue damage in the host (12–16). Therefore, understanding how round yeast-form cells become elongated hyphal cells and how these cells grow and respond to external physical and chemical stimuli is fundamental to understanding how *C. albicans* can transform from a benign commensal to an invasive pathogen. By quantifying the variations in the physical and mechanical properties of hyphae with high spatial resolution as they develop, we can gain a comprehensive understanding of how *C. albicans* cells colonize and invade surfaces, such as host tissues and implanted medical devices. Moreover, considering the limited classes of antifungal drugs available in the clinic and the enhanced resistance of fungal biofilms to these antifungal drugs, the ability to directly observe the effects of antifungal drugs on hyphal growth with high spatial resolution could be instrumental in the development of new antifungal therapies.

Despite their importance, directly visualizing morphological transitions of microbial cells with high spatial resolution and quantifying mechanical properties of different cellular morphologies under physiological conditions are an outstanding challenge in microbiology. Current methods (i.e., those based on electron microscopy and optical microscopy) often (i) involve complex sample preparation procedures (such as drying and staining), (ii) require specialized environments (such as a vacuum) that can lead to the degradation of samples from their natural states, and (iii) do not provide structural and mechanical information simultaneously. On the other hand, unlike other microscopy techniques, atomic force microscopy (AFM) is a unique imaging method that not only enables surface topography imaging of living cells with detailed spatial resolution under relevant environmental conditions (e.g., in liquid media) but also probes mechanical properties (e.g., stiffness and adhesion) with piconewton resolution in force without the need for preparation steps such as dehydration and labeling, thus preserving the natural state of biological samples.

AFM has been used in prior studies for both high-resolution imaging and mechanical property characterization of various microorganisms (17–24), including the fungal species *C. albicans* (25–30). In these studies, AFM was used to investigate the native states of the living microbial cells of interest in aqueous solutions using artificial cell immobilization procedures, such as trapping in porous membranes (23, 31), hydrogels (32, 33), or microfabricated microwells (34, 35), to avoid the detachment or movement of cells. The entrapment of cells with such artificial methods, however, can induce mechanical stresses that could lead to cell damage and modification of growth rates and mechanical properties, thus potentially biasing measurements (36). For instance, the formation of *C. albicans* hyphal cells could not be observed in previous AFM studies using firmly attached yeast cells by mechanical entrapment, suggesting that cell function and/or viability may have been compromised in these studies due to the use of artificial trapping methods.

Despite the sizeable number of prior AFM studies that use *C. albicans* cells, there are only a few studies that specifically focus on hyphal cells (25, 28, 37–42). In these studies, hyphae were grown from a culture for several hours and then immobilized on a substrate using either chemical fixation or hydrophobic coatings, and measurements were performed at room temperature either in buffered medium or under dry conditions. The use of AFM, however, for the direct imaging of the dynamic process of *C. albicans* hyphal formation using cells that have naturally adhered to a clinically relevant substrate without the need for any artificial immobilization techniques is yet to be shown.

To address this critical gap in knowledge, here we introduce an AFM-based approach to investigate dynamic hyphal growth in *C. albicans in situ* using liquid medium on silicone elastomer substrates, a clinically relevant material used in intravascular catheters. First, we investigate the influence of temperature on hyphal growth by
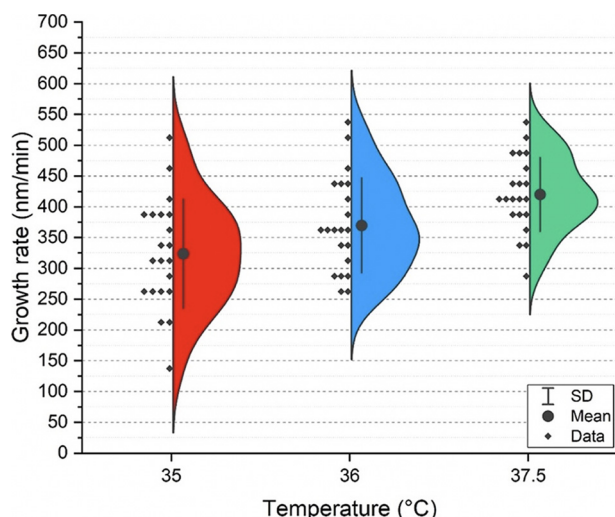
FIG 1 The effect of temperature on hyphal growth rates. Semiviolin plots depicting *C. albicans* hyphal growth rates with changing physiologically relevant temperatures in Spider medium.

taking successive AFM measurements at several physiologically relevant temperatures. Furthermore, we use AFM to explore the effects of antifungal drugs (caspofungin and fluconazole) on hyphal cell growth as well as to assess the mechanical properties of hyphal cell walls (using Young's [elastic] modulus and adhesion force) following treatment with antifungals. All of our experiments are performed at physiologically relevant temperatures of the human body and thus address a crucial drawback of prior *C. albicans* AFM studies that were performed at room temperature. Our results constitute the first direct *in situ* AFM study of unrestricted hyphal growth in *C. albicans* performed under physiologically relevant conditions and in the presence of commonly prescribed antifungal drugs, thus setting the framework for future mechanistic studies.

RESULTS

Effects of physiologically relevant temperatures on hyphal cell growth determined by AFM. We investigated the effect of temperature on growing hyphal cells (starting at germination) using successive AFM scans. The cells were scanned while growing on silicone elastomer substrates in Spider medium, a hyphal cell-inducing medium, at the physiologically relevant temperatures of 35°C, 36°C, and 37.5°C. For each temperature, 21 different hyphal cells, each from different culture batches, were scanned by AFM in tapping mode, and their growth rates were calculated (see Materials and Methods). Figure 1 shows the hyphal growth rate distributions in Spider medium at the three different temperatures assessed. The mean growth rate values were measured as 323.8 nm/min, 369.9 nm/min, and 420.1 nm/min at 35°C, 36°C, and 37.5°C, respectively.

Effects of antifungal drugs on hyphal cell growth determined by AFM. Since antifungal drugs are routinely used to treat *C. albicans* infections, we used AFM to investigate the growth of hyphal cells treated with fluconazole and caspofungin, two of the most commonly used antifungal drugs in the clinic. For these studies, newly germinated hyphal cells were grown on silicone elastomer substrates on the AFM sample stage for 20 min in Spider medium without drugs at 37.5°C. Spider medium without antifungal drugs was then exchanged for Spider medium containing 0.5 ng/ml of the antifungal drug fluconazole or caspofungin. Growth of hyphal cells (*n* = 4 cells for cells grown in the presence of fluconazole and *n* = 5 cells for cells grown in the presence of caspofungin, all from different starting cultures) was observed via consecutive AFM scans in tapping mode for 3 h at 37.5°C. Our results using hyphal cells demonstrate that they are more susceptible to fluconazole treatment (Fig. 2a) than caspofungin treatment (Fig. 2b). The growth rate of hyphal cells treated with flucona-
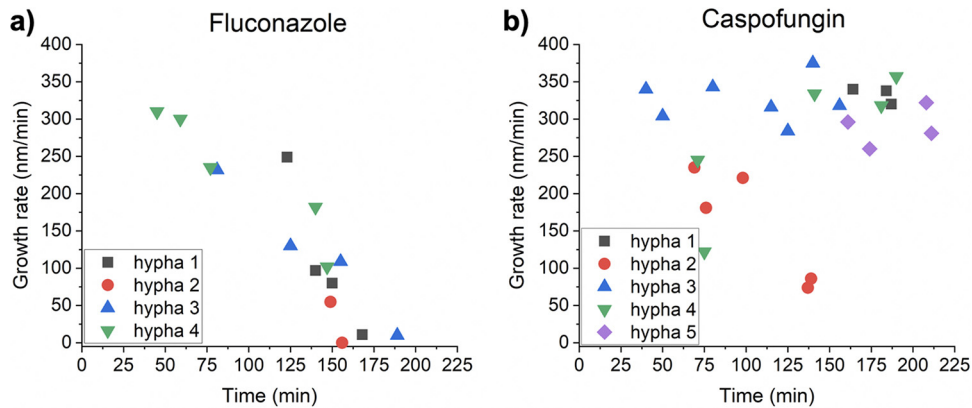
FIG 2 The effect of antifungal drugs on hyphal growth rates. (a) The evolution of growth rates in the presence of fluconazole. (b) The evolution of growth rates in the presence of caspofungin.

zole gradually decreased over time and nearly stopped after 3 h in the presence of fluconazole. When cells were exposed to caspofungin, however, few changes in overall hyphal growth rates were observed. Only one out of five hyphal cells showed a decrease in growth. Furthermore, compared to the ~420-nm/min average growth rate of hyphal cells at 37.5°C in drug-free medium (see the green semiviolin distribution in Fig. 1), in the presence of either antifungal drug (fluconazole or caspofungin), the average growth rate of hyphal cells was lower (~300 to 350 nm/min) after just ~40 min of drug exposure (Fig. 2a and b, ~40-min time point).

Hyphal cell wall stiffness in the presence of antifungal drugs. We next hypothesized that treatment of *C. albicans* with caspofungin or fluconazole would alter hyphal cell wall mechanics. Quantitative measurements of caspofungin- or fluconazole-induced mechanical variations on *C. albicans* hyphal cells have not been previously reported through the use of AFM. To test our hypothesis, we measured Young's moduli of growing *C. albicans* hyphal cells using AFM force-distance spectroscopy after treatment with caspofungin or fluconazole for 2 h at a concentration of 0.5 ng/ml. For each antifungal treatment, Young's moduli were determined as shown in Fig. 3a by fitting a Gaussian function to the overall histogram composed of all modulus values calculated from maps of 20 × 20 force-distance curves recorded on three different *C. albicans* hyphal cells grown from two independent cultures. We found that the mean Young's modulus of *C. albicans* hyphal cells had a value of 95.7 kPa (total number of recorded force curves, n = 505) prior to antifungal treatment, which is similar to previously published results (26, 43). After caspofungin treatment, the mean Young's modulus of
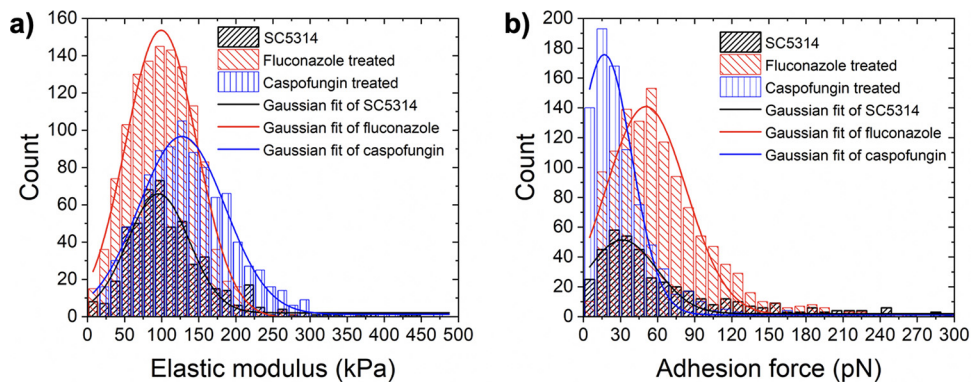

FIG 3 The effect of antifungal drugs on the mechanical properties of hyphal cell walls. Distribution of Young's (elastic) moduli (a) and adhesion forces (b) recorded on *C. albicans* hyphal cells prior to antifungal drug exposure (black bars) and after exposure to fluconazole (red bars) or caspofungin (blue bars).

C. albicans hyphal cells was increased by ~30% to a value of 127 kPa ($n = 954$). On the other hand, fluconazole-treated hyphal cells had nearly identical stiffness as untreated hyphal cells with a mean Young's modulus of 99.4 kPa ($n = 1,195$).

Adhesion force measurements of hyphal cells in the presence of antifungal drugs. To determine whether treatment with caspofungin or fluconazole can affect the strength of hyphal cell adherence, adhesion force measurements were performed on hyphal cells using AFM by recording maps of 20×20 force-distance curves. Three different *C. albicans* hyphal cells from two independent cultures were measured at 37.5°C after 2 h of treatment with caspofungin or fluconazole at concentrations of 0.5 ng/ml. Figure 3b shows the distribution of the measured adhesion forces of the *C. albicans* hyphal cells before and after treatment with the two antifungal drugs. The mean adhesion force of hyphal cells without antifungal treatment (total number of recorded force curves, $n = 504$) was 31.5 pN. After treatment with fluconazole, the mean adhesion force increased to 50.6 pN ($n = 1195$). In contrast, a decrease in the mean adhesion force to a value of 16.9 pN ($n = 884$) was observed for hyphal cells treated with caspofungin. Changes in adhesion induced by both antifungal drugs were statistically significant ($P < 0.0001$; calculated via Tukey's *post hoc* comparisons). We note that a direct comparison of adhesion forces reported here with those in the literature is not feasible given that bare AFM probes were utilized in our study whereas published results were obtained with probes functionalized with certain cells (38–40) or molecules (26, 27, 44).

Surface topography measurements of hyphal cells in the presence of antifungal drugs. To explore the effects of antifungal treatment on the surface topography of hyphal cells, we performed high-resolution AFM scans on hyphal cells in the presence and absence of caspofungin and fluconazole as reported in Fig. S1 in the supplemental material. We observed no significant changes in surface roughness or topography of hyphal cell walls upon treatment with fluconazole or caspofungin at the antifungal concentration used (0.5 ng/ml) (Fig. S1).

DISCUSSION

The ability of *C. albicans* cells to transition from yeast to hyphal forms is influenced by many environmental cues, including serum, *N*-acetylglucosamine, pH, carbon source, oxygen levels, and temperature (45–49). Hyphal cells are a critical component of *C. albicans* biofilms and are the morphological form that invades host epithelial cell layers to cause tissue damage and infections (50). Given the importance of the yeast-to-hyphal transition for virulence in the host, we investigated the effects of temperature on growing hyphal cells. Our results indicate that hyphal growth rates in Spider medium increase significantly with each incremental increase in temperature. Although this finding is not surprising given that physiological temperatures are known to induce hyphal formation, this is the first study to quantitatively evaluate such profound effects on hyphal growth as incremental physiological temperature adjustments occur. Given that the normal human body temperature fluctuates within these temperature ranges over the course of a 24-h period (51, 52), our findings indicate that minor body temperature changes within the normal range can markedly affect the morphology of *C. albicans* and thus significantly affect its pathogenic potential.

We also used AFM to investigate the growth of hyphal cells treated with fluconazole and caspofungin and found that hyphal cells are more susceptible to fluconazole than to caspofungin. The observation that fluconazole is more effective at suppressing hyphal growth compared to caspofungin is perhaps not surprising given that azoles block the synthesis of ergosterol, a major component of the fungal cell membrane (53). Caspofungin, on the other hand, inhibits the synthesis of cell wall β-1,3-D-glucans (54, 55) and may play a more central role in maintaining mechanical rigidity of the fungal cell wall. Therefore, we hypothesized that treatment of *C. albicans* with caspofungin would alter hyphal cell wall mechanics. There is some controversy in the literature regarding the mechanisms by which caspofungin impacts the mechanical properties of *C. albicans*. In one AFM study performed on *C. albicans* yeast-form cells, treatment with

caspofungin caused a softening of the cell wall (44), while other studies (26, 43) showed that Young's modulus, a measurement of stiffness, was increased following the treatment of *C. albicans* yeast-form cells with caspofungin. Based on the results we report here, we found that the mean Young's modulus of *C. albicans* hyphal cells was increased by ~30% after caspofungin treatment whereas fluconazole-treated hyphal cells had nearly identical stiffness as untreated hyphal cells. In *C. albicans*, inhibition of β-1,3-D-glucans by caspofungin treatment is known to result in an increase in the synthesis of chitin (56), a major polysaccharide that contributes to cell wall strength and can compensate for mechanical perturbations. Therefore, the cell wall stiffening we observe after caspofungin treatment is likely attributed to an increase in the amount of chitin in the hyphal cell wall (26, 43).

Other than the ability of *C. albicans* cells to undergo the yeast-to-hyphal transition, the ability of *C. albicans* cells to adhere to surfaces and form biofilms is another important virulence trait of this common human fungal pathogen. Adherence to surfaces is the first step in biofilm formation and is required for *C. albicans* cells to colonize host tissues and implanted medical devices (6, 28). As such, we investigated the effect of caspofungin and fluconazole treatments on adhesion measured via AFM on *C. albicans* hyphal cells. Our finding suggests that by significantly decreasing the adhesion forces of *C. albicans* cells attached to a surface, caspofungin is likely to be more effective than fluconazole in treating *C. albicans* biofilm infections in the clinic. Indeed, it is known that of the three major antifungal drugs commonly used in the clinic (caspofungin, fluconazole, and amphotericin B), caspofungin is the most effective against preformed *C. albicans* biofilms grown *in vitro*, while fluconazole is completely ineffective (57, 58).

It is feasible that differences in adhesion strength could be caused by drug-induced changes to the topography of the hyphal cell surface. The idea that caspofungin can cause changes to the *C. albicans* cell surface has been established in prior studies (44, 59, 60). However, we observed no significant changes in surface roughness or topography of hyphal cell walls upon treatment with fluconazole or caspofungin at the antifungal concentration used (see Fig. S1 in the supplemental material). It is possible that these antifungal drug concentrations were not adequate to induce damage to the hyphal cell walls and change the adhesion forces in that fashion.

In the absence of topographical changes that would explain the measured differences in *C. albicans* hyphal cell adhesion, the adherence of *C. albicans* cells to surfaces is likely mediated predominantly by adhesion molecules (adhesins) on the cell surface, such as the Als (agglutinin-like sequence) glycosylphosphatidylinositol (GPI)-anchored proteins (15, 61, 62). In fact, it was recently shown using AFM single-molecule analyses that high Als3 levels on the surface of hyphal cells promote cell adherence (37, 40). Taken together with our findings, it seems plausible that changes in adhesion forces upon treatment with caspofungin and fluconazole could correspond to variations in the expression of adhesin levels on the surfaces of hyphal cells. Nevertheless, further work needs to be performed at the single-molecule level to fully understand the physical and molecular reasons behind the effects of antifungal drugs on adhesion strength.

Finally, we note that the antifungal drug concentrations employed in this study are below the clinically relevant MIC values for caspofungin and fluconazole. These concentrations were chosen because they represent the highest antifungal drug concentrations that did not induce detachment of the fungal cells from the substrate. Despite this fact, our results demonstrate that even concentrations well below the MICs for these antifungal drugs have a measurable impact on hyphal growth and the mechanical properties of hyphal cells. This new information was not uncovered in previous AFM studies that solely focused on mechanically trapped yeast cells.

Here, we introduced for the first time the application of AFM for the *in situ* characterization of the growth dynamics and mechanical properties of *C. albicans* hyphal cells grown without entrapment on a clinically relevant material (silicone) at physiologically relevant temperatures. We showed that incremental changes in normal human body temperatures from 35°C to 37.5°C can have significant effects on hyphal

growth rates. Given that the normal human body temperature fluctuates within these temperature ranges over the course of a 24-h period, our findings indicate that minor body temperature changes within the normal range can markedly affect the morphology of *C. albicans* and thus significantly affect its pathogenic potential.

We also explored by AFM the effects of the most widely used antifungal drugs to treat *C. albicans* infections, caspofungin and fluconazole, on hyphal growth under physiologically relevant conditions. Our results showed that although caspofungin and fluconazole exposure did not significantly alter hyphal cell surface topography at concentrations of 0.5 ng/ml, treatment with fluconazole at the same concentration caused hyphal cell growth to cease after 3 h, while caspofungin had little to no impact on hyphal growth rates. Exposure to caspofungin and fluconazole also had different effects on the mechanical properties of hyphal cells. Hyphal cells exposed to caspofungin had increased stiffness and decreased adhesive strength relative to untreated hyphal cells and to fluconazole-treated hyphal cells. Interestingly, exposure to fluconazole also causes *C. albicans* hyphal cells to have increased adhesive strength relative to untreated hyphal cells. Overall, our results indicate that fluconazole and caspofungin have different effects on the growth and mechanical properties of *C. albicans* hyphal cells, which could impact the pathogenic potential of *C. albicans* in a host. These results also suggest that the combined or sequential use of fluconazole and caspofungin during treatment of *C. albicans* infections in the clinic could be beneficial when either drug used independently is ineffective. Overall, our findings set the stage for future studies aimed at uncovering the underlying physical and molecular mechanisms of the effects of temperature and antifungal drugs on *C. albicans* cells that could be further pursued with methods such as single-molecule force spectroscopy using AFM.

MATERIALS AND METHODS

Growth of *C. albicans* cells. *C. albicans* clinical reference strain SC5314 was used for all experiments. SC5314 was grown for 2 days at 30°C on yeast extract-peptone-dextrose (YPD) agar (1% yeast extract, 2% Bacto peptone, 2% dextrose, 2% agar). To prepare liquid cultures, a single colony was inoculated into YPD liquid medium and incubated overnight at 30°C with agitation at 225 rpm. *C. albicans* cells were harvested by centrifugation, washed three times with sterile phosphate-buffered saline (PBS) (pH 7.2), and resuspended in 1 ml of PBS buffer. Optical densities at 600 nm (OD_{600}) were measured and adjusted to ~19, and a 1:2,000 dilution of the cells was made in PBS. This dilution factor was chosen because it maintained a uniform distribution of cells on the silicone substrate at a low-enough density for proper AFM imaging.

Preparation of *C. albicans* cells on silicone elastomer substrates for AFM. To prevent cell detachment during AFM scans, squares of silicone elastomer substrates (1.5 by 1.5 cm) were cut from silicone sheets (Cardiovascular Instrument Corp.; PR72034-060N) and precoated with bovine serum as follows: silicone squares were washed in distilled and deionized water, dried, autoclaved, placed in sterile 12-well polystyrene non-tissue culture-treated plates (Corning; 351143), and then incubated with 2 ml of 1× fetal bovine serum (FBS) (Sigma-Aldrich) for 60 min at 37°C.

An 0.5-ml amount of the *C. albicans* cell solution was inoculated in 2 ml sterile Spider medium (63) (1% nutrient broth, 1% mannitol, 1% K_2PO_4, pH 7.2) at 37°C. The bovine serum-coated silicone elastomers were added into the *C. albicans* Spider medium cell solution and incubated for 20 min at 37°C with agitation at 200 rpm in an ELMI digital thermostatic shaker. At the end of this procedure, *C. albicans* cells initiated hyphal formation (germ tubes were on the order of 5 μm in length) on the silicone elastomer substrates (see Fig. S2).

Imaging the growth of *C. albicans* hyphal cells by AFM. Surface topography scans and growth rate measurements of *C. albicans* hyphal cells were carried out with an Asylum Research Cypher VRS atomic force microscope (Santa Barbara, CA, USA). Liquid Spider medium at temperatures varying between 35°C and 37.5°C was used, depending on the specific experiment. Silicon nitride cantilevers with silicon tips (Olympus; BL-AC40TS; nominal spring constant $k = 0.1$ N/m) were used in all experiments. Prior to the experiments, the normal spring constant of each cantilever was determined from the first resonance frequency (which was around 27 kHz in buffer solution) of the thermal noise spectra using the GetReal calibration procedure integrated into the AFM software.

The silicone elastomer substrate with *C. albicans* germ tubes was attached to a steel sample puck using double-sided tape. The mounted elastomer was transferred onto the heating stage of the AFM, which was already set to a temperature between 35°C and 37.5°C, depending on the experiment. The silicone substrate containing *C. albicans* germ tubes was washed 3 times with 100 ml Spider medium to remove unattached cells. Twenty milliliters of Spider medium at 37°C was drop-cast onto the silicone surface before performing topographical scans via tapping mode of AFM in liquid. Once a suitable region with cells that had initiated hyphal formation was found with the optical camera of the AFM, the cantilever was approached, and an initial scan was made over an area of 25 μm by 25 μm with a scan rate of 0.30 Hz. A consecutive scan of the same area was then performed at the same scan speed. Figure S3

shows representative, consecutive topographical images of a growing *C. albicans* hyphal cell recorded as described above.

Calculating the growth rates of *C. albicans* hyphal cells. After AFM images were processed with the scanning probe microscopy data analysis software package Gwyddion 2.53 (64), height profiles along the longitudinal directions of a particular hyphal cell were studied in successive AFM scans (see Fig. S3) to calculate hyphal growth in terms of the apex-to-apex distance between the line profiles being compared, as shown representatively in Fig. S3c. The elapsed time associated with apex-to-apex growth of a hyphal cell was calculated from the total number of scanned lines between apexes in consecutive AFM scans and the scan time per line. Finally, the growth rate was calculated as the ratio of the growth between apexes in AFM scans and the time elapsed to scan the apex-to-apex growth by AFM.

For the hyphal cell shown as an example in Fig. S3, the scan rate was 0.25 Hz (i.e., each image was composed of 256 lines recorded in 17.1 min). Therefore, apex-to-apex growth of the hyphal cell in consecutive scans was recorded in 27.7 min for 414 scanned lines (i.e., 202 lines from Fig. S3a and 212 lines from Fig. S3b). Hence, the growth rate of this hyphal cell is 300 nm/min for a total of 8,300 nm of growth, calculated from the comparison of line profiles in Fig. S3c.

Measuring adhesion forces and Young's moduli of *C. albicans* hyphal cells via AFM force-distance spectroscopy. Prior to force measurements, substrates were briefly imaged in tapping mode, first over a large area (e.g., 30 μm in lateral size) to find hyphal cells, and then over a small area (e.g., 400 nm in lateral size) to focus on a location at the middle regions of a growing hyphal cell (see Fig. S4). To probe adhesion forces and elastic moduli of hyphal cells, maps of 20×20 force-distance curves were recorded on scanned areas (see Fig. S5) of the hyphal cell with an Asylum Research Cypher VRS atomic force microscope (Santa Barbara, CA, USA) in Spider medium at 37°C with BL-AC40TS cantilevers (Olympus; $k = 0.1$ N/m, $f = 27$ kHz in liquid), which were calibrated prior to the experiments as described above. To record the interaction forces between the AFM probe and the hyphal cell of interest as a function of the distance between them, the probe was approached to and then retracted from the hyphal cell at a constant speed of 1,000 nm/s. Force-distance curves were recorded on three different hyphal cells from two independent cultures of *C. albicans*, with a maximum applied force of 250 pN to ensure the indentation was lower than 10% of hyphal cell height to avoid cross talk with the mechanical properties of the substrate (65).

To convert AFM force-distance curves to force-indentation curves, each force-distance curve on the force maps was processed by correcting the baseline offset and tilt of the curves and by subtracting the effects of cantilever bending using the Igor Pro software (WaveMetrics Inc.). From the force-indentation curves, the adhesion force of each curve was calculated as the lowest negative rupture force recorded when retracting the tip from the surface of the hyphal cell of interest. The measured adhesion force values are presented as pixelated maps in Fig. S5d to f, and statistical distributions for these values are shown in Fig. 3b. The mean calculated adhesion force of each statistical distribution was determined by fitting a Gaussian function to the overall histogram composed of all measured adhesion force values.

The elastic stiffness of hyphal cells can be deduced from the approach segment of the force-indentation curves. After processing the force-distance curves, the characteristic power-law shape of the approach segment was fitted to the Hertz model (66) for a paraboloid tip geometry to estimate Young's modulus, E. The Hertz model describes the deformation behavior of purely linear elastic materials (67). Biological samples are never perfectly linearly elastic but are instead viscoelastic with a short range of linear elasticity (68). Several studies have shown that for small indentation depths and for small indenters compared to sample dimensions, the force-indentation data follow Hertzian mechanics (69–71). Therefore, to ensure data are extracted from the linearly elastic regime, experiments were performed for shallow indentation depths up to 100 nm with a maximum force of 250 pN. The results are shown as pixelated two-dimensional (2D) maps in Fig. S5a to c, and statistical distributions of Young's moduli values are shown in Fig. 3a.

Data availability. The data that support the findings of this study are available from the corresponding authors upon request.

SUPPLEMENTAL MATERIAL

Supplemental material is available online only.

FIG S1, TIF file, 0.8 MB.
FIG S2, TIF file, 0.7 MB.
FIG S3, TIF file, 0.7 MB.
FIG S4, TIF file, 0.2 MB.
FIG S5, TIF file, 0.4 MB.

ACKNOWLEDGMENTS

REFERENCES

1. Kullberg BJ, Oude Lashof AM. 2002. Epidemiology of opportunistic invasive mycoses. Eur J Med Res 7:183–191.
2. Kim J, Sudbery P. 2011. *Candida albicans*, a major human fungal pathogen. J Microbiol 49:171–177. https://doi.org/10.1007/s12275-011-1064-7.
3. Calderone RA, Clancy CJ. 2012. Candida and candidiasis, 2nd ed. ASM Press, Washington, DC.
4. Douglas LJ. 2003. Candida biofilms and their role in infection. Trends Microbiol 11:30–36. https://doi.org/10.1016/s0966-842x(02)00002-1.
5. Sardi JCO, Scorzoni L, Bernardi T, Fusco-Almeida AM, Mendes Giannini MJS. 2013. Candida species: current epidemiology, pathogenicity, biofilm formation, natural antifungal products and new therapeutic options. J Med Microbiol 62:10–24. https://doi.org/10.1099/jmm.0.045054-0.
6. Nobile CJ, Johnson AD. 2015. *Candida albicans* biofilms and human disease. Annu Rev Microbiol 69:71–92. https://doi.org/10.1146/annurev-micro-091014-104330.
7. Lohse MB, Gulati M, Johnson AD, Nobile CJ. 2018. Development and regulation of single- and multi-species *Candida albicans* biofilms. Nat Rev Microbiol 16:19–31. https://doi.org/10.1038/nrmicro2017.107.
8. Donlan RM, Costerton JW. 2002. Biofilms: survival mechanisms of clinically relevant microorganisms. Clin Microbiol Rev 15:167–193. https://doi.org/10.1128/cmr.15.2.167-193.2002.
9. Gulati M, Nobile CJ. 2016. *Candida albicans* biofilms: development, regulation, and molecular mechanisms. Microbes Infect 18:310–321. https://doi.org/10.1016/j.micinf.2016.01.002.
10. Chandra J, Kuhn DM, Mukherjee PK, Hoyer LL, McCormick T, Ghannoum MA. 2001. Biofilm formation by the fungal pathogen *Candida albicans*: development, architecture, and drug resistance. J Bacteriol 183:5385–5394. https://doi.org/10.1128/jb.183.18.5385-5394.2001.
11. Ramage G, Saville SP, Thomas DP, López-Ribot JL. 2005. Candida biofilms: an update. Eukaryot Cell 4:633–638. https://doi.org/10.1128/EC.4.4.633-638.2005.
12. Brand A. 2012. Hyphal growth in human fungal pathogens and its role in virulence. Int J Microbiol 2012:517529. https://doi.org/10.1155/2012/517529.
13. Gow NA. 1997. Germ tube growth of *Candida albicans*. Curr Top Med Mycol 8:43–55.
14. Gow NAR, Brown AJP, Odds FC. 2002. Fungal morphogenesis and host invasion. Curr Opin Microbiol 5:366–371. https://doi.org/10.1016/S1369-5274(02)00338-7.
15. Gow NAR, van de Veerdonk FL, Brown AJ, Netea MG. 2011. *Candida albicans* morphogenesis and host defence: discriminating invasion from colonization. Nat Rev Microbiol 10:112–122. https://doi.org/10.1038/nrmicro2711.
16. Gow NAR, Hube B. 2012. Importance of the *Candida albicans* cell wall during commensalism and infection. Curr Opin Microbiol 15:406–412. https://doi.org/10.1016/j.mib.2012.04.005.
17. Snijder J, Radtke K, Anderson F, Scholtes L, Corradini E, Baines J, Heck AJR, Wuite GJL, Sodeik B, Roos WH. 2017. Vertex-specific proteins pUL17 and pUL25 mechanically reinforce herpes simplex virus capsids. J Virol 91:e00123-17. https://doi.org/10.1128/JVI.00123-17.
18. Mathelié-Guinlet M, Asmar AT, Collet JF, Dufrêne YF. 2020. Lipoprotein Lpp regulates the mechanical properties of the *E. coli* cell envelope. Nat Commun 11:1789. https://doi.org/10.1038/s41467-020-15489-1.
19. Lekka M, Pabijan J. 2019. Measuring elastic properties of single cancer cells by AFM. Methods Mol Biol 1886:315–324. https://doi.org/10.1007/978-1-4939-8894-5_18.
20. Dufrêne YF, Boonaert CJ, Gerin PA, Asther M, Rouxhet PG. 1999. Direct probing of the surface ultrastructure and molecular interactions of dormant and germinating spores of *Phanerochaete chrysosporium*. J Bacteriol 181:5350–5354. https://doi.org/10.1128/JB.181.17.5350-5354.1999.
21. Canetta E, Adya AK, Walker GM. 2006. Atomic force microscopic study of

the effects of ethanol on yeast cell surface morphology. FEMS Microbiol Lett 255:308–315. https://doi.org/10.1111/j.1574-6968.2005.00089.x.
22. Dague E, Alsteens D, Latgé JP, Dufrêne YF. 2008. High-resolution cell surface dynamics of germinating Aspergillus fumigatus conidia. Biophys J 94:656–660. https://doi.org/10.1529/biophysj.107.116491.
23. Alsteens D, Dupres V, Mc Evoy K, Wildling L, Gruber HJ, Dufrêne YF. 2008. Structure, cell wall elasticity and polysaccharide properties of living yeast cells, as probed by AFM. Nanotechnology 19:384005. https://doi.org/10.1088/0957-4484/19/38/384005.
24. El-Kirat-Chatel S, Beaussart A, Derclaye S, Alsteens D, Kucharíková S, Van Dijck P, Dufrêne YF. 2015. Force nanoscopy of hydrophobic interactions in the fungal pathogen Candida glabrata. ACS Nano 9:1648–1655. https://doi.org/10.1021/nn506370f.
25. El-Kirat-Chatel S, Dufrêne YF. 2012. Nanoscale imaging of the *Candida*-macrophage interaction using correlated fluorescence-atomic force microscopy. ACS Nano 6:10792–10799. https://doi.org/10.1021/nn304116f.
26. Hasim S, Allison DP, Retterer ST, Hopke A, Wheeler RT, Doktycz MJ, Reynolds TB. 2017. β-(1,3)-Glucan unmasking in some *Candida albicans* mutants correlates with increases in cell wall surface roughness and decreases in cell wall elasticity. Infect Immun 85:e00601-16. https://doi.org/10.1128/IAI.00601-16.
27. Murillo LA, Newport G, Lan CY, Habelitz S, Dungan J, Agabian NM. 2005. Genome-wide transcription profiling of the early phase of biofilm formation by *Candida albicans*. Eukaryot Cell 4:1562–1573. https://doi.org/10.1128/EC.4.9.1562-1573.2005.
28. Aguayo S, Marshall H, Pratten J, Bradshaw D, Brown JS, Porter SR, Spratt D, Bozec L. 2017. Early adhesion of *Candida albicans* onto dental acrylic surfaces. J Dent Res 96:917–923. https://doi.org/10.1177/0022034517706354.
29. Bhat SV, Sultana T, Körnig A, McGrath S, Shahina Z, Dahms TES. 2018. Correlative atomic force microscopy quantitative imaging-laser scanning confocal microscopy quantifies the impact of stressors on live cells in real-time. Sci Rep 8:8305. https://doi.org/10.1038/s41598-018-26433-1.
30. Tokarska-Rodak M, Czernik S, Chwedczuk M, Plewik D, Grudniewski T, Pawłowicz-Sosnowska ET. 2019. The analysis of nanomechanical properties of Candida spp. by atomic force microscopy (AFM) method. Postepy Hig Med Dosw 73:353–358. https://doi.org/10.5604/01.3001.0013.3449.
31. Kasas S, Ikai A. 1995. A method for anchoring round shaped cells for atomic force microscope imaging. Biophys J 68:1678–1680. https://doi.org/10.1016/S0006-3495(95)80344-9.
32. Gad M, Ikai A. 1995. Method for immobilizing microbial cells on gel surface for dynamic AFM studies. Biophys J 69:2226–2233. https://doi.org/10.1016/S0006-3495(95)80147-5.
33. De T, Chettoor AM, Agarwal P, Salapaka MV, Nettikadan S. 2010. Immobilization method of yeast cells for intermittent contact mode imaging using the atomic force microscope. Ultramicroscopy 110:254–258. https://doi.org/10.1016/j.ultramic.2009.12.003.
34. Dague E, Jauvert E, Laplatine L, Viallet B, Thibault C, Ressier L. 2011. Assembly of live micro-organisms on microstructured PDMS stamps by convective/capillary deposition for AFM bio-experiments. Nanotechnology 22:395102. https://doi.org/10.1088/0957-4484/22/39/395102.
35. Formosa C, Pillet F, Schiavone M, Duval RE, Ressier L, Dague E. 2015. Generation of living cell arrays for atomic force microscopy studies. Nat Protoc 10:199–204. https://doi.org/10.1038/nprot.2015.004.
36. Alsteens D. 2012. Microbial cells analysis by atomic force microscopy. Methods Enzymol 506:3–17. https://doi.org/10.1016/B978-0-12-391856-7.00025-1.
37. Beaussart A, Alsteens D, El-Kirat-Chatel S, Lipke PN, Kucharíková S, Van Dijck P, Dufrêne YF. 2012. Single-molecule imaging and functional anal-

ysis of Als adhesins and mannans during *Candida albicans* morphogenesis. ACS Nano 6:10950–10964. https://doi.org/10.1021/nn304505s.

38. Ovchinnikova ES, Krom BP, Busscher HJ, van der Mei HC. 2012. Evaluation of adhesion forces of *Staphylococcus aureus* along the length of *Candida albicans* hyphae. BMC Microbiol 12:281. https://doi.org/10.1186/1471-2180-12-281.

39. Ovchinnikova ES, Krom BP, van der Mei HC, Busscher HJ. 2012. Force microscopic and thermodynamic analysis of the adhesion between Pseudomonas aeruginosa and Candida albicans. Soft Matter 8:6454–6461. https://doi.org/10.1039/c2sm25100k.

40. Alsteens D, Van Dijck P, Lipke PN, Dufrêne YF. 2013. Quantifying the forces driving cell-cell adhesion in a fungal pathogen. Langmuir 29:13473–13480. https://doi.org/10.1021/la403237f.

41. Beaussart A, Herman P, El-Kirat-Chatel S, Lipke PN, Kucharíková S, Van Dijck P, Dufrêne YF. 2013. Single-cell force spectroscopy of the medically important *Staphylococcus epidermidis-Candida albicans* interaction. Nanoscale 5:10894–10900. https://doi.org/10.1039/c3nr03272h.

42. Ma S, Ge W, Yan Y, Huang X, Ma L, Li C, Yu S, Chen C. 2017. Effects of *Streptococcus sanguinis* bacteriocin on deformation, adhesion ability, and Young's modulus of *Candida albicans*. Biomed Res Int 2017:5291486. https://doi.org/10.1155/2017/5291486.

43. Formosa C, Schiavone M, Martin-Yken H, François JM, Duval RE, Dague E. 2013. Nanoscale effects of caspofungin against two yeast species, *Saccharomyces cerevisiae* and *Candida albicans*. Antimicrob Agents Chemother 57:3498–3506. https://doi.org/10.1128/AAC.00105-13.

44. El-Kirat-Chatel S, Beaussart A, Alsteens D, Jackson DN, Lipke PN, Dufrêne YF. 2013. Nanoscale analysis of caspofungin-induced cell surface remodelling in *Candida albicans*. Nanoscale 5:1105–1115. https://doi.org/10.1039/c2nr33215a.

45. Taschdjian CL, Burchall JJ, Kozinn PJ. 1960. Rapid identification of *Candida albicans* by filamentation on serum and serum substitutes. AMA J Dis Child 99:212–215. https://doi.org/10.1001/archpedi.1960.02070030214011.

46. Simonetti N, Strippoli V, Cassone A. 1974. Yeast-mycelial conversion induced by N-acetyl-D-glucosamine in *Candida albicans*. Nature 250:344–346. https://doi.org/10.1038/250344a0.

47. Buffo J, Herman MA, Soll DR. 1984. A characterization of pH-regulated dimorphism in *Candida albicans*. Mycopathologia 85:21–30. https://doi.org/10.1007/BF00436698.

48. Klengel T, Liang WJ, Chaloupka J, Ruoff C, Schröppel K, Naglik JR, Eckert SE, Mogensen EG, Haynes K, Tuite MF, Levin LR, Buck J, Mühlschlegel FA. 2005. Fungal adenylyl cyclase integrates CO_2 sensing with cAMP signaling and virulence. Curr Biol 15:2021–2026. https://doi.org/10.1016/j.cub.2005.10.040.

49. Shapiro RS, Uppuluri P, Zaas AK, Collins C, Senn H, Perfect JR, Heitman J, Cowen LE. 2009. Hsp90 orchestrates temperature-dependent *Candida albicans* morphogenesis via Ras1-PKA signaling. Curr Biol 19:621–629. https://doi.org/10.1016/j.cub.2009.03.017.

50. Noble SM, Gianetti BA, Witchley JN. 2017. *Candida albicans* cell-type switching and functional plasticity in the mammalian host. Nat Rev Microbiol 15:96–108. https://doi.org/10.1038/nrmicro.2016.157.

51. Mackowiak PA, Wasserman SS, Levine MM. 1992. A critical appraisal of 98.6 degrees F, the upper limit of the normal body temperature, and other legacies of Carl Reinhold August Wunderlich. JAMA 268:1578–1580. https://doi.org/10.1001/jama.1992.03490120092034.

52. Kelly G. 2006. Body temperature variability (part 1): a review of the history of body temperature and its variability due to site selection, biological rhythms, fitness, and aging. Altern Med Rev 11:278–293.

53. Kathiravan MK, Salake AB, Chothe AS, Dudhe PB, Watode RP, Mukta MS, Gadhwe S. 2012. The biology and chemistry of antifungal agents: a review. Bioorg Med Chem 20:5678–5698. https://doi.org/10.1016/j.bmc.2012.04.045.

54. Douglas CM, D'Ippolito JA, Shei GJ, Meinz M, Onishi J, Marrinan JA, Li W, Abruzzo GK, Flattery A, Bartizal K, Mitchell A, Kurtz MB. 1997. Identifica-

tion of the FKS1 gene of *Candida albicans* as the essential target of 1,3-beta-D-glucan synthase inhibitors. Antimicrob Agents Chemother 41:2471–2479. https://doi.org/10.1128/AAC.41.11.2471.

55. Letscher-Bru V, Herbrecht R. 2003. Caspofungin: the first representative of a new antifungal class. J Antimicrob Chemother 51:513–521. https://doi.org/10.1093/jac/dkg117.

56. Walker LA, Munro CA, de Bruijn I, Lenardon MD, McKinnon A, Gow NAR. 2008. Stimulation of chitin synthesis rescues *Candida albicans* from echinocandins. PLoS Pathog 4:e1000040. https://doi.org/10.1371/journal.ppat.1000040.

57. Bachmann SP, VandeWalle K, Ramage G, Patterson TF, Wickes BL, Graybill JR, López-Ribot JL. 2002. In vitro activity of caspofungin against *Candida albicans* biofilms. Antimicrob Agents Chemother 46:3591–3596. https://doi.org/10.1128/aac.46.11.3591-3596.2002.

58. Ramage G, VandeWalle K, Bachmann SP, Wickes BL, López-Ribot JL. 2002. In vitro pharmacodynamic properties of three antifungal agents against preformed *Candida albicans* biofilms determined by time-kill studies. Antimicrob Agents Chemother 46:3634–3636. https://doi.org/10.1128/aac.46.11.3634-3636.2002.

59. Bizerra FC, Melo ASA, Katchburian E, Freymüller E, Straus AH, Takahashi HK, Colombo AL. 2011. Changes in cell wall synthesis and ultrastructure during paradoxical growth effect of caspofungin on four different Candida species. Antimicrob Agents Chemother 55:302–310. https://doi.org/10.1128/AAC.00633-10.

60. Dunyach C, Drakulovski P, Bertout S, Jouvert S, Reynes J, Mallié M. 2011. Fungicidal activity and morphological alterations of *Candida albicans* induced by echinocandins: study of strains with reduced caspofungin susceptibility. Mycoses 54:e62–e68. https://doi.org/10.1111/j.1439-0507.2009.01834.x.

61. Dranginis AM, Rauceo JM, Coronado JE, Lipke PN. 2007. A biochemical guide to yeast adhesins: glycoproteins for social and antisocial occasions. Microbiol Mol Biol Rev 71:282–294. https://doi.org/10.1128/MMBR.00037-06.

62. Hoyer LL. 2001. The *ALS* gene family of *Candida albicans*. Trends Microbiol 9:176–180. https://doi.org/10.1016/s0966-842x(01)01984-9.

63. Liu H, Kohler J, Fink GR. 1994. Suppression of hyphal formation in *Candida albicans* by mutation of a STE12 homolog. Science 266:1723–1726. https://doi.org/10.1126/science.7992058.

64. Nečas D, Klapetek P. 2012. Gwyddion: an open-source software for SPM data analysis. Cent Eur J Phys 10:181–188.

65. Krieg M, Fläschner G, Alsteens D, Gaub BM, Roos WH, Wuite GJL, Gaub HE, Gerber C, Dufrêne YF, Müller DJ. 2019. Atomic force microscopy-based mechanobiology. Nat Rev Phys 1:41–57. https://doi.org/10.1038/s42254-018-0001-7.

66. Hertz H. 1882. Über die Berührung fester elastischer Körper. J Reine Angew Math 92:156–171. https://doi.org/10.1515/crll.1882.92.156.

67. Johnson KL, Kendall K, Roberts AD. 1971. Surface energy and the contact of elastic solids. Proc R Soc Lond 324:301–313. https://doi.org/10.1098/rspa.1971.0141.

68. McKee CT, Last JA, Russell P, Murphy CJ. 2011. Indentation versus tensile measurements of Young's modulus for soft biological tissues. Tissue Eng Part B Rev 17:155–164. https://doi.org/10.1089/ten.TEB.2010.0520.

69. Faria EC, Ma N, Gazi E, Gardner P, Brown M, Clarke NW, Snook RD. 2008. Measurement of elastic properties of prostate cancer cells using AFM. Analyst 133:1498–1500. https://doi.org/10.1039/b803355b.

70. Zhou ZL, Ngan AHW, Tang B, Wang AX. 2012. Reliable measurement of elastic modulus of cells by nanoindentation in an atomic force microscope. J Mech Behav Biomed Mater 8:134–142. https://doi.org/10.1016/j.jmbbm.2011.11.010.

71. Lekka M. 2016. Discrimination between normal and cancerous cells using AFM. Bionanoscience 6:65–80. https://doi.org/10.1007/s12668-016-0191-3.